ISTITUTO NAZIONALE
DI GEOFISICA E VULCANOLOGIA

INGV SPACE WEATHER BULLETIN OVER THE MEDITERRANEAN AREA

ISTITUTO NAZIONALE
DI GEOFISICA E VULCANOLOGIA

INGV SPACE WEATHER BULLETIN OVER THE MEDITERRANEAN AREA

Issue nr. 17/2024

From 15-Apr-2024 to 21-Apr-2024

Generated on 22-Apr-2024

INGV Ambiente | The Space Weather Monitoring Group*

Introduction **4**

1. Summary of the week **5**

2. Solar Activity **6**

2.1 X-Ray Flux monitoring 6

2.2 Proton Flux monitoring 7

2.3 Solar Wind and Interplanetary Magnetic Field monitoring 8

3. Ionospheric Activity **9**

3.1 HF data 9

3.2 TEC data 12

3.3 GNSS Scintillation data 15

4. Geomagnetic Activity **19**

4.1 Geomagnetic observatories time series 20

4.2 Planetary Kp index 21

4.3 Local K index at Duronia observatory 22

4.4 Disturbance Storm Time Dst Index 23

Acknowledgments and Data Policy **24**

Introduction

The INGV weekly Space Weather report over the Mediterranean area is prepared by the Space Weather Monitoring Group (SWMG) which operates in the INGV Environment Department. The aim of the SWMG is to monitor the Sun and Sun-Earth environment conditions in order to promptly communicate, mainly via social media, the occurrence of Space Weather related events potentially harmful for technology and society. Furthermore, the SWMG is devoted to outreach the general public with information and highlights about Space Weather related topics and science, either with "pills" on the main social media (Facebook, Instagram and Twitter), and with occasional insights published on the INGV Environment Department Blog.

As a summary of the monitoring activities, the SWMG produces this weekly report, focusing on the observations from the facilities that INGV handles in Italy and in the Mediterranean area. These geomagnetic and ionospheric observatories and stations are represented in Figure 1 below along with the INGV RING network of geodetic receivers, which also provide useful ionospheric data.

An overview of the solar activity as the Space Weather driver is given in Section 2. Such data do not come from INGV observations but are shown by courtesy of the Space Weather Prediction Center of the U.S. National Oceanic and Atmospheric Administration (SWPC-NOAA).

All the INGV Space Weather Bulletins can be found at the Roma2 webpage following the path from the homepage: "Monitoring and Surveillance >> Monitoring products >> Space Weather Bulletins" (or directly at this link).

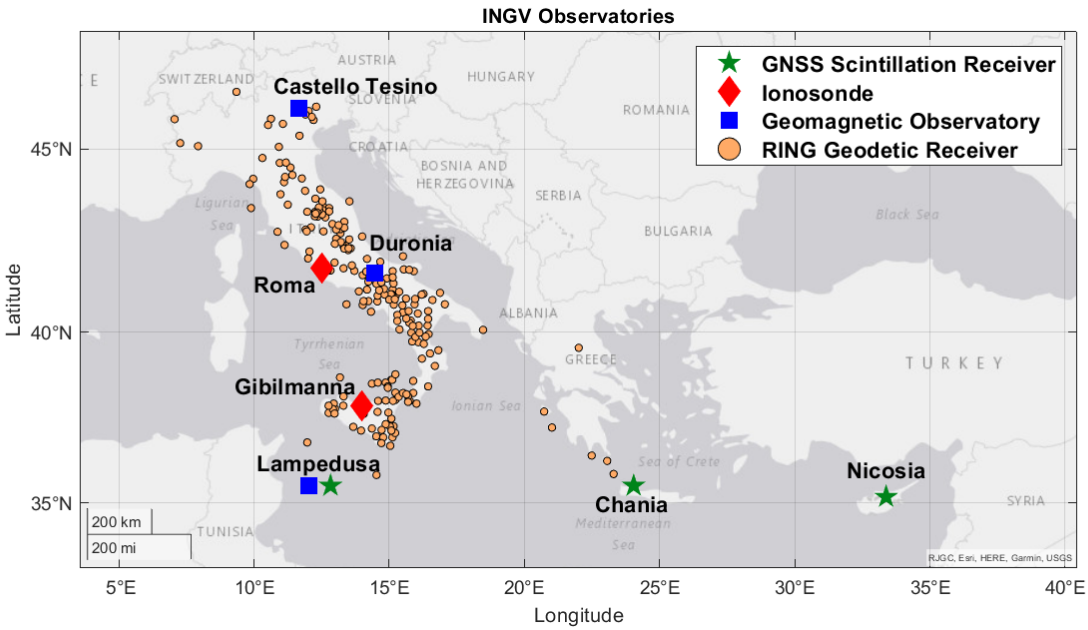

Figure 1: Locations of the INGV observatories and measuring stations which acquire data useful for Space Weather purposes.

1. Summary of the week

The week was characterized by two geomagnetic storms, as visible from the Dst index, occurring between 16 and 17 April and between 19 and 22 April. The latter, being the most intense between the two (maximum Kp=7 at 18 UTC of 19 April, minimum Dst=-122 nT at 19 UTC of 19 April) is still in its recovery phase. The Local K index at Duronia observatory reached a maximum value of 6 at the same time of the Kp peak.

The disturbed geomagnetic conditions resulted in ionospheric storm signatures affecting almost the entire week. Specifically, positive TEC storm signatures are found from the morning UTC hours of 15 April until the morning of 21 April. In correspondence with the main phase of the first geomagnetic storm, negative foF2 storm deviations are found for Rome (while Gibilmanna is characterized by a partial lack of data), while in correspondence with the main phase of the second geomagnetic storm, positive foF2 deviations are found for both Rome (between 00 and 12 UTC on 20 April) and Gibilmanna (between 12 on 19 April and 12 UTC on 20 April).

For what concerns the scintillation activity, the three receivers in Lampedusa, Chania, and Nicosia recorded scintillation events during the week. Specifically, the Lampedusa receiver recorded scintillation events during the evening and nighttime hours, local post sunset hours of 15, 16 and 18 April. The latter event was also recorded in Nicosia and Chania, while that of 16 April recorded in Lampedusa lasted until the early morning hours (01 UTC) of 17 April. All those scintillation events are ascribable to the presence of post-sunset equatorial plasma bubbles entering the field of view of the receivers.

In Figure 2, an overview of the overall Space Weather activity during the week is depicted: every 12 hours (UTC time reported on the horizontal axis), a summary of the parameters which gave out-of-threshold values is shown. When a parameter in a given time window exceeds the threshold for an event, the corresponding box is colored in dark red, while black boxes represent time windows with no data available. More details on the values exceeding the thresholds and the meaning of the observed parameters are given in the following sections.

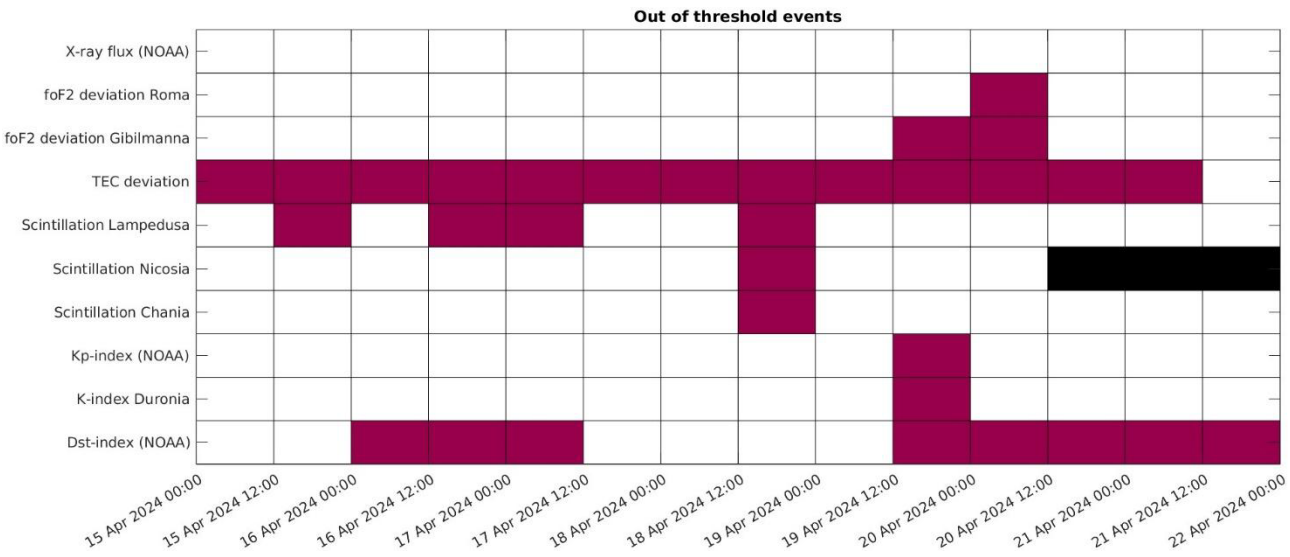

Figure 2: Summary of measurements which reported out-of-threshold events (red boxes) and lack of data (black ones) during the week.

2. Solar Activity

2.1 X-Ray Flux monitoring

During solar flares, bursts of electromagnetic radiation are emitted in space, in a wide spectrum of frequencies ranging from radio waves to gamma rays. To Space Weather purposes, the most dangerous part of such radiation is constituted by X rays, having wavelengths between about 0.5 to 8 Å. The NOAA geosynchronous satellites GOES-16 and GOES-18, measure the X-Ray flux coming to Earth. A solar flare can be classified by the intensity of the emitted X-Ray flux: the threshold set by NOAA for having an alert of possible dangerous events is “M5”, corresponding to an X-ray flux of $5 \cdot 10^{-5}$ W/m^2.

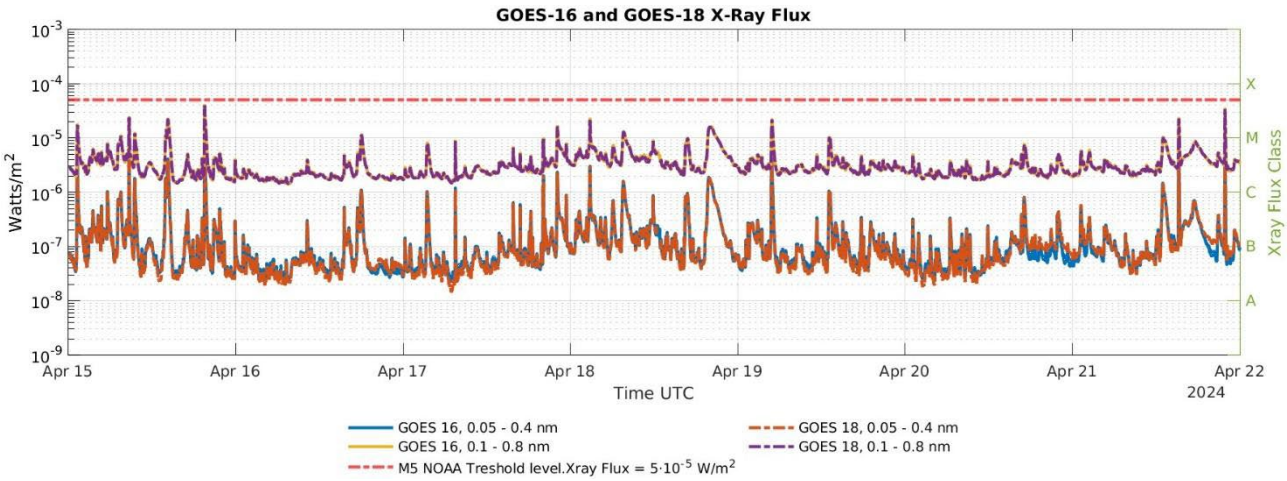

Figure 3: X-ray flux coming from the Sun as measured by GOES-16 and GOES-18 NOAA satellites.

Table I: Flares M5 class or higher

Event List	Event start time (UT)	Event stop time (UT)	Time of max (UT)	Detected max value
"No event"	"No event"	"No event"	"No event"	"No event"

2.2 Proton Flux monitoring

Among Space Weather phenomena, Solar Particle Events (SPEs) can also occur: particles emitted by the Sun, mostly protons, become accelerated either in the Sun's atmosphere during a solar flare or in interplanetary space by a coronal mass ejection shock. Again, the GOES-16 and GOES-18 satellites measure the flux of solar protons and NOAA fixes a threshold of 10 particles/($cm^2 \cdot s \cdot sr$) for the 10 MeV proton flux in order to raise an alert.

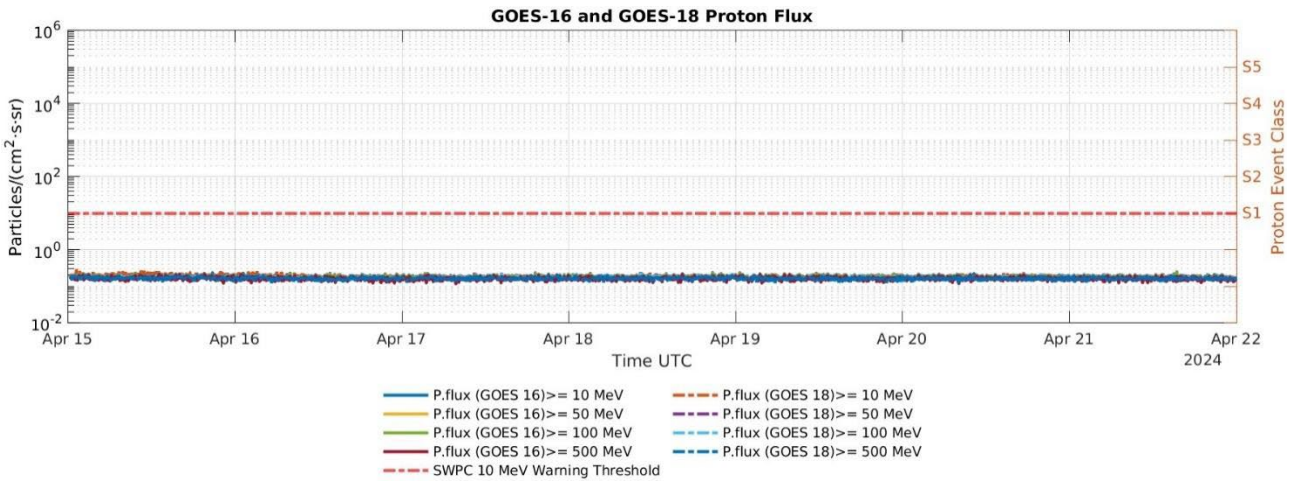

Figure 4: Solar proton's flux measured by GOES-16 and GOES-18 NOAA satellites.

2.3 Solar Wind and Interplanetary Magnetic Field monitoring

Coronal Mass Ejections (CMEs) can push interplanetary shocks close to Earth. A pair of NASA satellites located at the Lagrangian L1 point (1.5 million km along the Sun-Earth direction), ACE and DSCOVR, are devoted to monitor Interplanetary Magnetic Field (IMF) and Solar Wind (i.e., the continuous stream of charged particles that flow from the Sun) parameters in order to spot events that can have an impact on Earth, about 30-60 minutes in advance. Particularly important to monitor is the B_z component of IMF: if it has a negative sign for long periods the IMF can couple with the Earth's magnetic field and let more energy and solar wind particles penetrate the magnetospheric cavity. The solar wind state is monitored through the measure of its density and velocity.

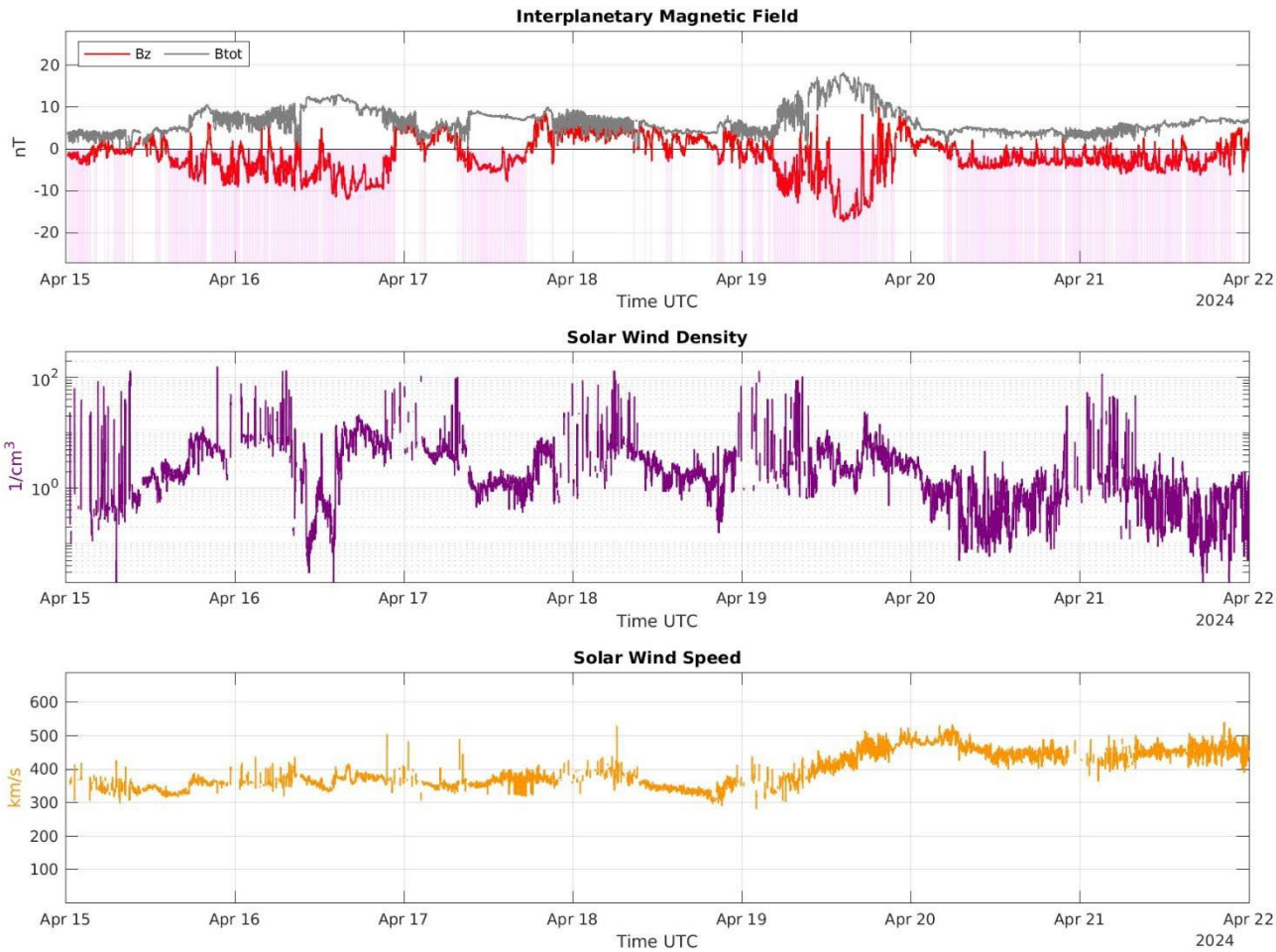

Figure 5: Top panel: Interplanetary Magnetic Field B_z (red) component e total field (black); Middle panel: Solar Wind density; Bottom panel: Solar Wind speed. Measures come from NASA DISCVR spacecraft, or NASA ACE spacecraft if DISCVR data are not available.

3. Ionospheric Activity

3.1 HF data

Under active Space Weather conditions, extra energy is deposited into the high-latitude ionosphere, possibly triggering ionospheric storms at planetary scale, with positive or negative effects in the ionization. At the INGV ionospheric stations of Rome (41.8°N; 12.5°E) and Gibilmanna (37.9°N; 14.0°E), ground-based high frequency (HF) radio soundings are routinely performed, measuring ionospheric parameters directly related to the ionization level, which could affect HF radio communications. A decreased ionization may indeed lower the upper limit of the working frequency band for such communications. The critical frequency of the F2 layer, foF2, proportional to the peak value of the electron density over the sounding location, and the Maximum Usable Frequency for radio communications over a standard distance of 3000 km, MUF(3000)F2, are continuously monitored through automatic scaling in real-time of the ionograms recorded routinely at the INGV ionospheric observatories. The foF2 hourly-averaged relative deviation from its median over the previous 27 days allows to quantify the severity of the perturbation and the corresponding effect on the HF communications. The thresholds of ±20% and ±40% deviations are used to characterize moderate and severe effects respectively, and to raise alerts when severe conditions occur.

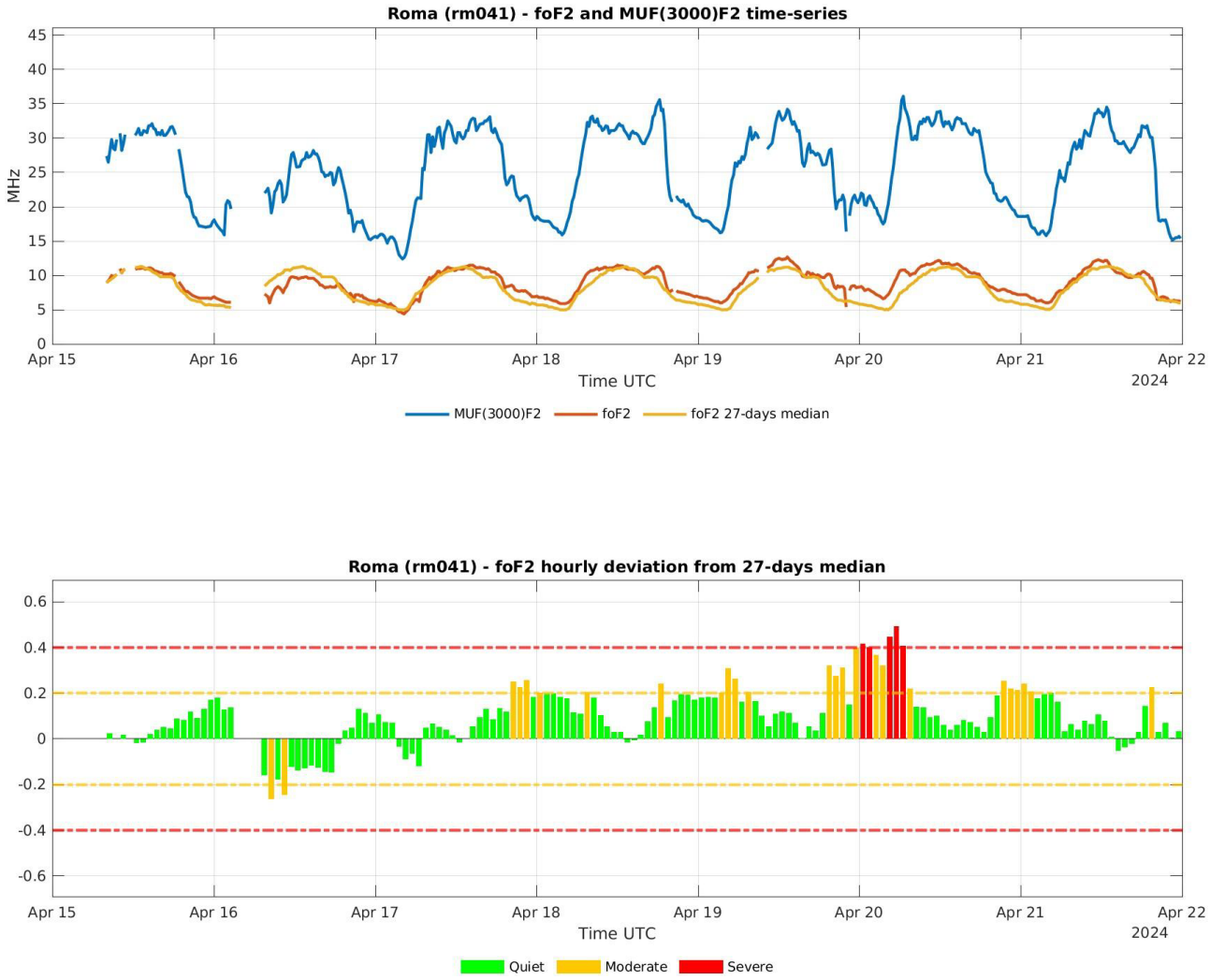

Figure 6: HF data from the INGV ionospheric observatory of Rome. Top panel: foF2 (orange), corresponding median over the previous 27 days (yellow), and MUF(3000)F2 (blue); Bottom panel: foF2 hourly-averaged relative deviation from 27-days median, with colors (green, yellow and red) associated to the severity of the perturbation, according to the ±0.2 and ±0.4 thresholds reported with horizontal yellow and red dashed lines, respectively.

Table II: Rome - foF2 hourly deviation Severe events

Event List	Event start time (UT)	Event stop time (UT)	Time of max (UT)	Detected max value
1	"2024-04-20 00:00"	"2024-04-20 02:00"	"2024-04-20 00:00"	0.4154
2	"2024-04-20 04:00"	"2024-04-20 07:00"	"2024-04-20 05:00"	0.4931

Figure 7: Same as Fig. 6 for the HF data from the INGV ionospheric observatory of Gibilmanna.

Table III: Gibilmanna – foF2 hourly deviation Severe events

Event List	Event start time (UT)	Event stop time (UT)	Time of max (UT)	Detected max value
1	"2024-04-19 23:00"	"2024-04-20 03:00"	"2024-04-20 01:00"	0.5119
2	"2024-04-20 04:00"	"2024-04-20 07:00"	"2024-04-20 05:00"	0.5049

3.2 TEC data

The presence of free electrons and ions in the Earth's upper atmosphere is mainly due to the ionizing action of solar radiation. The TEC (Total Electron Content) is the total number of electrons in a cylinder with a base of one square meter and which has the height of the imaginary segment that connects a transmitter, for example a Global Navigation Satellite Systems (GNSS) satellite, and a receiver on the ground. It is typically expressed in TEC units (1 TECu=10^{16} e/m^2). Radio waves are affected by the presence of electrons: the more electrons in the path of the radio wave, the more the radio signal will be affected. For ground-to-satellite communications and satellite navigation, the TEC is a good metric to monitor possible impacts from Space Weather. The bulletin reports the average TEC calculated over the Italian area (5°E-20°E; 35°N-48°N) as well as the hourly-averaged relative deviation of the mean TEC from its median over the previous 27 days, allowing to quantify the severity of the disruption. The thresholds of ±20% and ±40% deviations are used to characterize moderate and severe effects respectively, and to raise alerts when severe conditions occur. The TEC data are generated by processing the real-time data of the geodetic receivers of the INGV RING network.

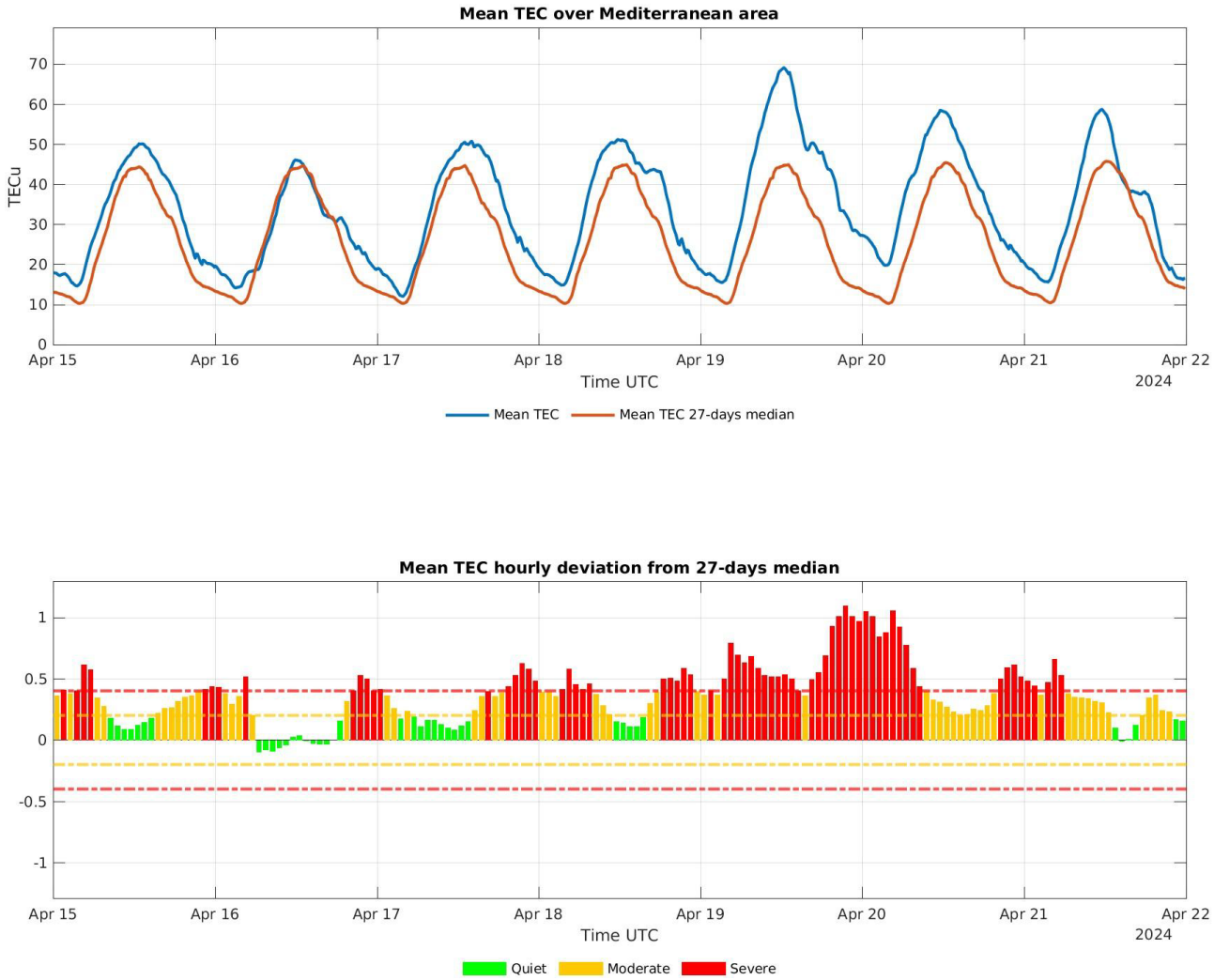

Figure 8: Top panel: mean TEC over the Italian area (blue) from data of the receivers of the INGV RING network, and corresponding median over the previous 27 days (orange); Bottom panel: mean TEC hourly-averaged relative deviation from 27-days median, with colors (green, yellow and red) associated to the severity of the perturbation, according to the ±0.2 and ±0.4 thresholds reported with horizontal yellow and red dashed lines, respectively.

Table IV: TEC hourly deviation Severe events

Event List	Event start time (UT)	Event stop time (UT)	Time of max (UT)	Detected max value
1	"2024-04-15 01:00"	"2024-04-15 02:00"	"2024-04-15 01:00"	0.4087
2	"2024-04-15 03:00"	"2024-04-15 06:00"	"2024-04-15 04:00"	0.6171
3	"2024-04-15 22:00"	"2024-04-16 01:00"	"2024-04-15 23:00"	0.4394
4	"2024-04-16 04:00"	"2024-04-16 05:00"	"2024-04-16 04:00"	0.5209
5	"2024-04-16 20:00"	"2024-04-17 01:00"	"2024-04-16 21:00"	0.5273
6	"2024-04-17 16:00"	"2024-04-17 17:00"	"2024-04-17 16:00"	0.4005
7	"2024-04-17 19:00"	"2024-04-18 00:00"	"2024-04-17 21:00"	0.6257
8	"2024-04-18 03:00"	"2024-04-18 08:00"	"2024-04-18 04:00"	0.5818
9	"2024-04-18 18:00"	"2024-04-18 23:00"	"2024-04-18 21:00"	0.5871
10	"2024-04-19 01:00"	"2024-04-19 02:00"	"2024-04-19 01:00"	0.4015
11	"2024-04-19 03:00"	"2024-04-19 15:00"	"2024-04-19 04:00"	0.7957

Event List	Event start time (UT)	Event stop time (UT)	Time of max (UT)	Detected max value
12	"2024-04-19 16:00"	"2024-04-20 09:00"	"2024-04-19 21:00"	1.0935
13	"2024-04-20 20:00"	"2024-04-21 02:00"	"2024-04-20 22:00"	0.6153
14	"2024-04-21 03:00"	"2024-04-21 06:00"	"2024-04-21 04:00"	0.6594

3.3 GNSS Scintillation data

The ionosphere can present electron density irregularities that can cause diffraction and refraction of radio signals passing through it. The fluctuations of signals emitted by GNSS satellites, both in amplitude and phase, induced by diffractive phenomena are called ionospheric scintillations. Ionospheric scintillations can cause serious problems to satellite signals by compromising, for example, the precision and accuracy of positioning provided by navigation systems. The formation, evolution and dynamics of these irregularities are determined by the interaction between the geomagnetic field, the ionospheric currents, the IMF and the solar wind and are the manifestation of different physical phenomena depending on the latitude at which they occur. The bulletin reports the hourly maximum values of the amplitude scintillation index (S4) recorded by 3 INGV receivers for GNSS scintillation located in the Mediterranean area. The thresholds of moderate ($0.25<S4<0.7$) and severe ($S4>0.7$) scintillations are used to characterize the severity of the GNSS scintillation events.

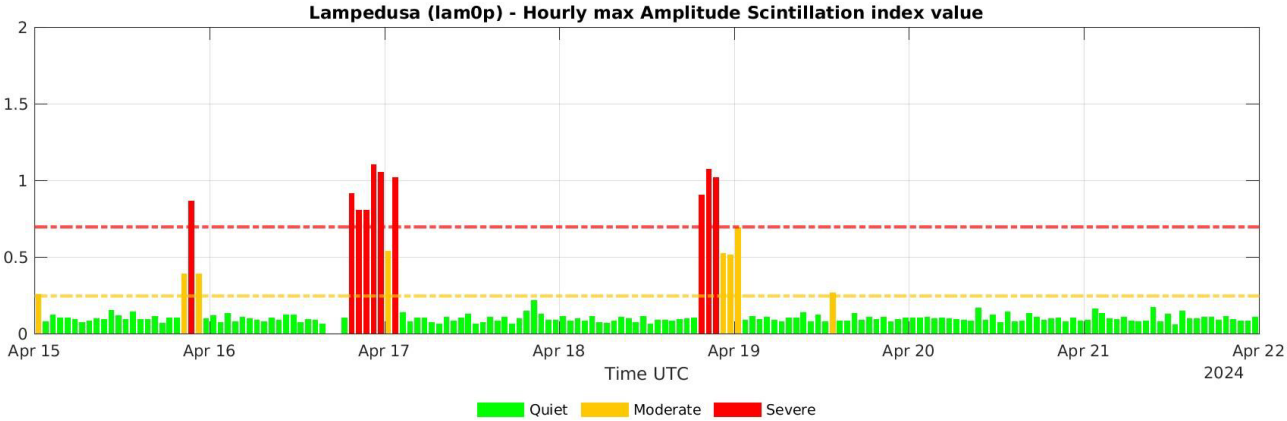

Figure 9: S4 hourly maximum values recorded by the INGV receiver for GNSS scintillation located in Lampedusa, with colors (green, yellow and red) associated to the severity of the scintillation, according to the 0.25 and 0.7 thresholds reported with horizontal yellow and red dashed lines, respectively.

Table V: Lampedusa – Amplitude Scintillation Severe events

Event List	Event start time (UT)	Event stop time (UT)	Time of max (UT)	Detected max value
1	"2024-04-15 21:00"	"2024-04-15 22:00"	"2024-04-15 21:00"	0.8679
2	"2024-04-16 19:00"	"2024-04-17 00:00"	"2024-04-16 22:00"	1.1055
3	"2024-04-17 01:00"	"2024-04-17 02:00"	"2024-04-17 01:00"	1.0234
4	"2024-04-18 19:00"	"2024-04-18 22:00"	"2024-04-18 20:00"	1.0753

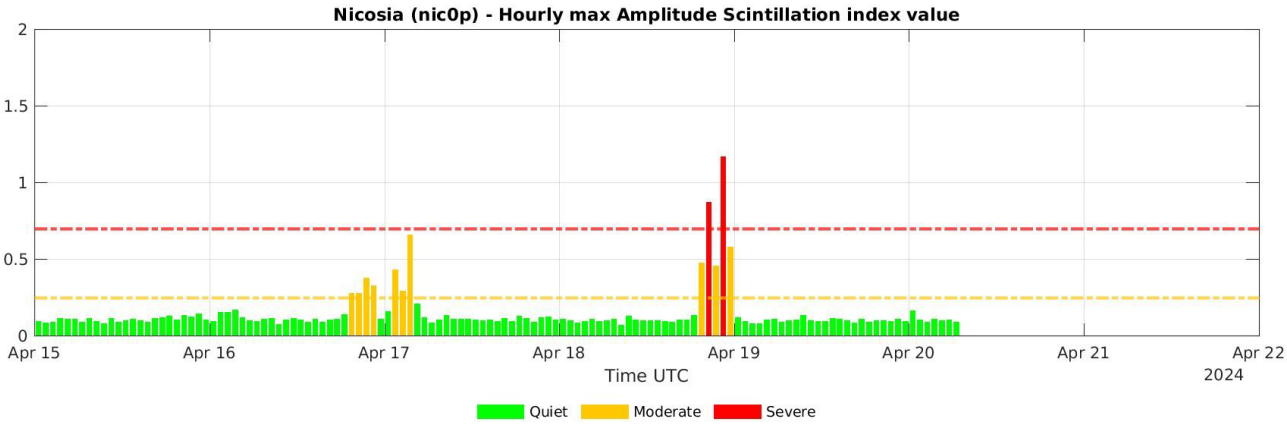

Figure 10: Same as Figure 9 for the data from the INGV receiver for GNSS scintillation located in Nicosia.

Table VI: Nicosia - Amplitude Scintillation Severe events

Event List	Event start time (UT)	Event stop time (UT)	Time of max (UT)	Detected max value
1	"2024-04-18 20:00"	"2024-04-18 21:00"	"2024-04-18 20:00"	0.8733
2	"2024-04-18 22:00"	"2024-04-18 23:00"	"2024-04-18 22:00"	1.1684

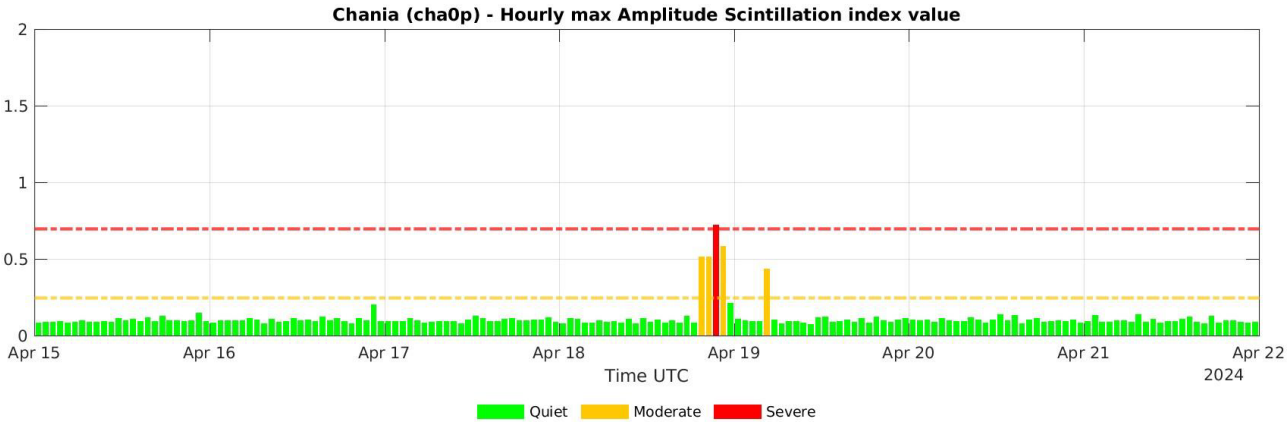

Figure 11: Same as Figure 9 for the data from the INGV receiver for GNSS scintillation located in Chania.

Table VII: Chania - Amplitude Scintillation Severe events

Event List	Event start time (UT)	Event stop time (UT)	Time of max (UT)	Detected max value
1	"2024-04-18 21:00"	"2024-04-18 22:00"	"2024-04-18 21:00"	0.7259

4. Geomagnetic Activity

Geomagnetic observatories are important infrastructures for monitoring space weather changes because their signature is present in the Earth's magnetic field, which is directly influenced by solar activity. The magnetic field of the Earth is constantly interacting with the Solar Wind and with the solar magnetic field which is transported by it. Changes in the solar wind parameters can cause disturbances in the Earth's magnetic field and in the ionosphere. These disturbances can result in a range of space weather effects on Earth, including magnetic and ionospheric storms, auroras, and disruptions of power grids and satellite communications.

By continuously monitoring the Earth's magnetic field, geomagnetic observatories can provide early warning of potential Space Weather hazards, helping scientists to better understand the physics of the interactions between the Sun and the Earth's magnetic field. Data from multiple observatories around the world allow researchers to build a more comprehensive picture of Space Weather patterns and develop more accurate models for predicting Space Weather effects.

4.1 Geomagnetic observatories time series

Focusing on the three geomagnetic observatories in Italy (Castello Tesino, Duronia and Lampedusa, from north to south), visual inspection of the stacking of the magnetograms related to the horizontal component H (in nT) at each site reveals many featuring of the global character of a magnetic storm, like the time of the storm's trigger in case of sharp commencement, duration of the storm, rapidity of variations and relative intensity. Statistical comparison of individual behavior in quiet/disturbed conditions gives the empirical weighted scale to categorize the grade of the magnetic activity.

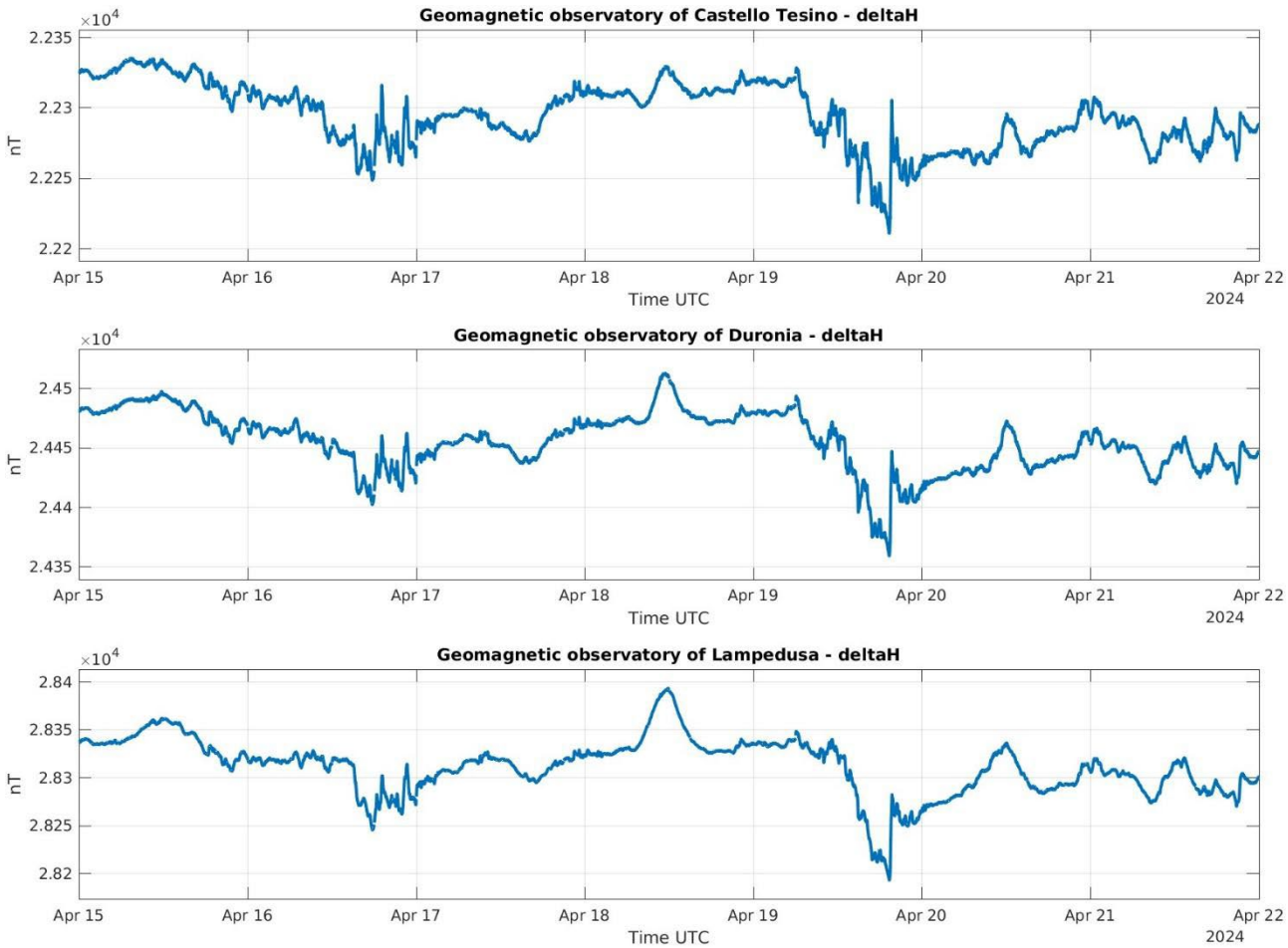

Figure 12: Magnetograms showing the variation of the horizontal component of the Earth's magnetic field at the Italian geomagnetic observatories (Castello Tesino, Duronia and Lampedusa from top to bottom).

4.2 Planetary Kp index

The Kp index is an indicator of disturbances in the Earth's magnetic field and it can be used for characterizing the geomagnetic activity aimed at generating alerts and warnings that need to be issued for users who are affected by these disturbances. It quantifies disturbances in the horizontal component with an integer in the range 0-9 with 1 being calm and 5 or more indicating a geomagnetic storm. It is derived as an average value from the maximum fluctuations of horizontal components observed in three-hour intervals on 13 selected magnetometers, whose 11 located in the northern hemisphere and 2 in the southern hemisphere, between 44° and 60° northern or southern geomagnetic latitude. The estimated 3-hour Planetary Kp-index is derived by the NOAA Space Weather Prediction Center.

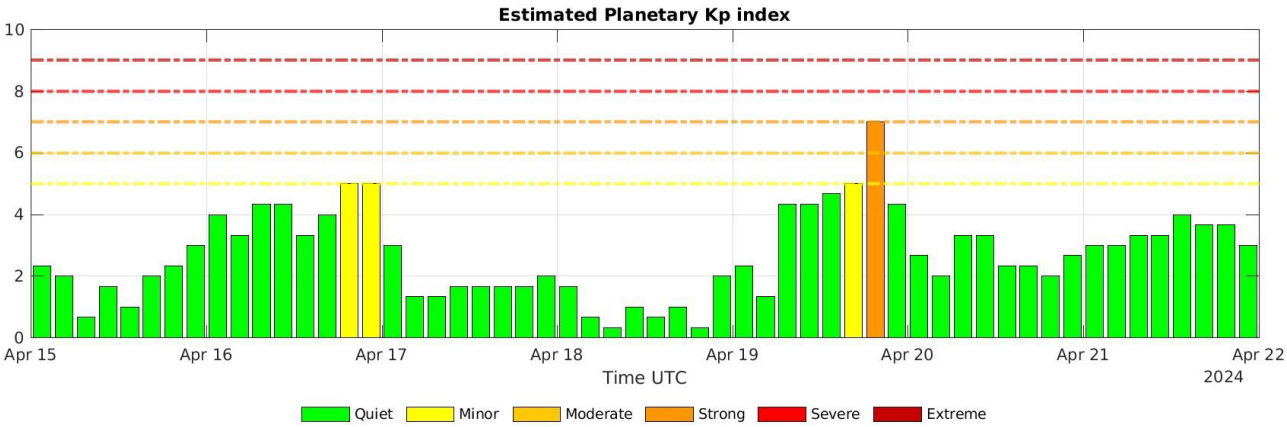

Figure 13: HIstogram of Kp index released by NOAA. Coloured bars indicate the intensity of the global magnetic activity on Earth, according to the corresponding thresholds.

Table VIII: Estimated Planetary Kp index above Moderate threshold events

Event List	Event start time (UT)	Event stop time (UT)	Time of max (UT)	Detected max value
1	"2024-04-19 18:00"	"2024-04-19 21:00"	"2024-04-19 18:00"	7

4.3 Local K index at Duronia observatory

Local K index at Duronia observatory is fully equivalent to the Kp index above described. It is based on the horizontal component of the Earth's magnetic field recorded at Duronia, and it manifests a slight difference with respect to the planetary index, being this latter an averaged value, and moreover local K index reflects the individual geologic/tectonic response from the site. Local K indexes from the other two observatories are practically equivalent to the Duronia K index.

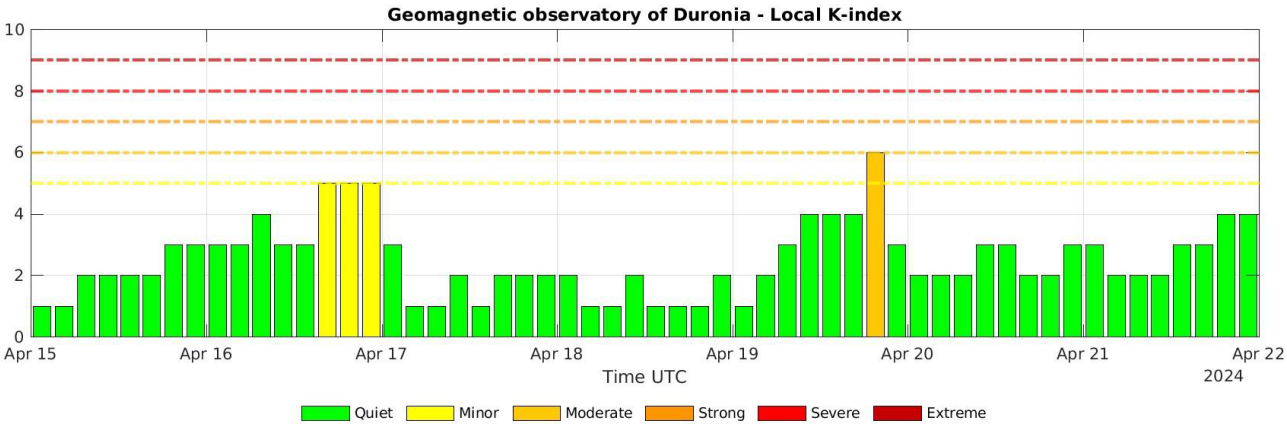

Figure 14: As in Figure 13, histogram of local K index based on the magnetic field recorded at Duronia geomagnetic observatory.

Table IX: Duronia - Local K index above Moderate threshold events

Event List	Event start time (UT)	Event stop time (UT)	Time of max (UT)	Detected max value
1	"2024-04-19 18:00"	"2024-04-19 21:00"	"2024-04-19 18:00"	6

4.4 Disturbance Storm Time Dst Index

The Dst index is used as a proxy of the intensity of the ring current, even if it is actually influenced by the axially symmetric portion of all magnetospheric currents (including the tail currents and the magnetopause Chapman-Ferraro current). It is estimated using 1-hour values from four low latitude observatories (sufficiently distant from the auroral and equatorial electrojets to inhibit noise from these two sources) and often used to characterize the evolution of a geomagnetic storm. Its unit is the nanoTesla (nT) since it measures the disturbance on the horizontal component of the Earth's magnetic field due to variations in intensity (mainly) of the ring current. The Dst index here published is the real-time version, suitable only for monitoring, since estimated from unverified raw geomagnetic data. The Dst index is estimated from the World Data Center of Geomagnetism (Kyoto, Japan). Data are taken from the NOAA Space Weather Prediction Center.

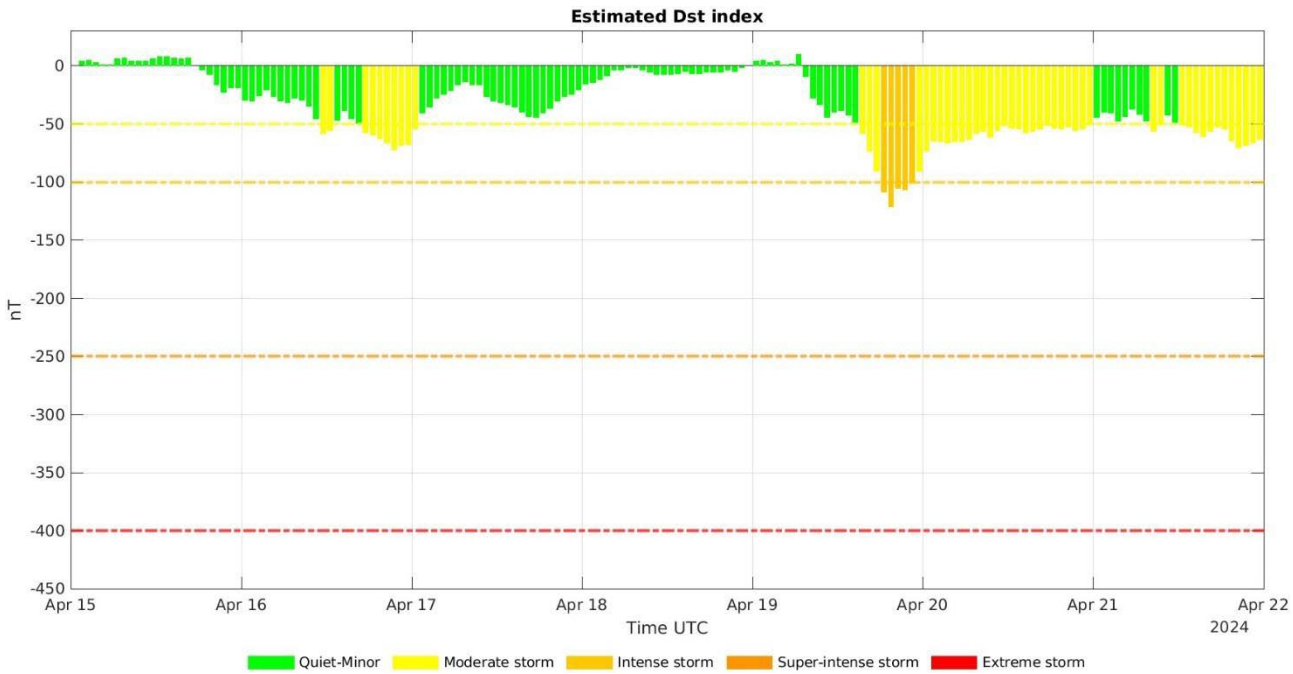

Figure 15: Histogram of Dst index taken from NOAA. Coloured bars indicate the intensity of the disturbance of the ring current, according to the corresponding thresholds.

Table X: Estimated Dst index above Moderate threshold events

Event List	Event start time (UT)	Event stop time (UT)	Time of max (UT)	Detected max value
1	"2024-04-16 11:00"	"2024-04-16 13:00"	"2024-04-16 11:00"	-59
2	"2024-04-16 16:00"	"2024-04-17 01:00"	"2024-04-16 21:00"	-73
3	"2024-04-19 15:00"	"2024-04-21 00:00"	"2024-04-19 19:00"	-122
4	"2024-04-21 08:00"	"2024-04-21 10:00"	"2024-04-21 08:00"	-57
5	"2024-04-21 12:00"	"2024-04-22 00:00"	"2024-04-21 20:00"	-71

Acknowledgments and Data Policy

- Data related to Sun and solar wind monitoring (Section 2), as well as Kp and Dst indices data (Sections 4.2 and 4.4), are taken from the Space Weather Prediction Center (SWPC) of the U.S. National Oceanic and Atmospheric Administration (NOAA). Dst index is estimated from the World Data Center of Geomagnetism (Kyoto, Japan). The information is in the public domain, unless specifically noted otherwise, as detailed in their Disclaimer.

The INGV SWMG thanks the SWPC at NOAA for making data available.

- The ionospheric and geomagnetic data upon which Sections 3 and 4 of this bulletin are based, are owned by the Istituto Nazionale di Geofisica e Vulcanologia (INGV) and distributed under a Creative Commons Attribution 4.0 International (CC BY 4.0).

You are free to:
Share — copy and redistribute the material in any medium or format.
Adapt — remix, transform, and build upon the material for any purpose, even commercially.

Nevertheless, **you must** give appropriate credit to the data owner and to the INGV SWMG by adding the following acknowledgement to your publications and material based on this bulletin:

"We thank the Italian "Istituto Nazionale di Geofisica e Vulcanologia (INGV)" and the INGV Space Weather Monitoring Group for providing the data/information [specify which data/information] we have used in our work."

- The ionospheric observatories raw and elaborated data are distributed through the INGV "electronic Space Weather upper atmosphere" (eSWua) portal.

- The TEC data are generated by processing the real-time data of the geodetic receivers of the INGV RING network.

- The geomagnetic observatories raw and elaborated data are distributed through the "Geomagnetic INGV data portal".

In any case, any risk due to improper use of these data falls under the responsibility of the individual user. In no case and way INGV will be responsible for direct, indirect, voluntary or accidental damages, including lost profits, deriving from the use of the data even if INGV was advised of this possibility.

***The Space Weather Monitoring Group (SWMG) of INGV Environment Department:**

Igino Coco, Tommaso Alberti, Paolo Bagiacchi, Lili Cafarella, Claudio Cesaroni, Gianfranco Cianchini, Domenico Di Mauro, Fabio Giannattasio, Alessandro Ippolito, Carlo Marcocci, Loredana Perrone, Michael Pezzopane, Emanuele Pica, Alessio Pignalberi, Vincenzo Romano, Dario Sabbagh, Carlo Scotto, Sabina Spadoni, Luca Spogli, Roberta Tozzi, Massimo Viola

Graphic and editorial design support by Barbara Angioni

For questions and information please contact: INGVAmbiente.SWbulletin@ingv.it